ELSEVIER

Journal of Power Sources 53 (1995) 45–51

JOURNAL OF POWER SOURCES

Hardening process in ternary lead–antimony–tin alloys for battery grids

J.P. Hilger

Laboratoire de Thermodynanique Métallurgique CNRS ER 78, Université Henri Poincaré, Nancy I, BP 239, 54506 Vandoeuvre-lès-Nancy Cedex, France

Received 27 July 1994; accepted 12 August 1994

Abstract

It is known that lead–antimony alloys are very well hardened by continuous precipitation, whereas lead–tin alloys present a discontinuous precipitation with a weak hardening effect. In these binary alloys, there is precipitation of either antimony or tin. In ternary alloys, the compound SbSn can also precipitate. This study is focused on the type of precipitation, the nature and the morphology of the precipitated phases, and the intensity of hardening in ternary Pb–Sb–Sn alloys in relation to the composition of the alloys and the ternary diagram. To simulate the different processes of grid production, four states are studied, namely, as-cast product, rehomogenized, cold worked, cold worked and rehomogenized. The alloys contain up to 2.5 wt.% Sb and 2.5 wt.% Sn.

Keywords: Lead–antimony–tin alloys; Lead hardening process; Discontinuous and continuous transformation; Lead–antimony–tin diagram

1. Introduction

The traditional alloys for grids in lead/acid batteries have been based on the lead–antimony system. The use of low-antimony alloys has become important for low-maintenance batteries. These alloys, however, have lower castability and a reduced ability to age-hardening. A small addition of tin improves the fluidity and the castability. Lead–calcium–tin alloys with low tin contents suffer from passivation (the 'antimony-free effect'). To reduce this phenomenon, plating with a thin Pb–Sb–Sn alloy layer has been recommended [1].

The present work is concerned with the age-hardening process in ternary Pb–Sb–Sn alloys in relation to the composition of the alloys and the ternary phase diagram. To simulate the different processes of grid production (i.e. gravity cast, continuous cast, rolled expanded [2,3] and cast expanded [4–6] grids), four initial states are systematically studied, viz., as-cast product, rehomogenized and water quenched, cold rolled, cold rolled and rehomogenized.

2. Experimental

2.1. Alloy composition

Lead–antimony–tin alloys were melted at 500 °C. The alloys were synthesized by dissolution of primary lead, pure antimony and pure tin in a bath of Pb–2.5 wt.% Sb alloy that was contained in an SiO_2 crucible with an 8-mm diameter. The samples were water quenched in the crucible in order to simulate the cooling conditions of battery grids.

All the compositions are represented in the ternary Pb–Sb–Sn diagram, Fig. 1. No selenium or arsenic was added.

2.2. Thermomechanical treatment

For all compositions, the cast samples were divided into four pieces: as-cast; rehomogenized; rolled; rolled then rehomogenized. The rehomogenization was generally performed at 280 °C for 15 min. All the samples were aged at room temperature for one year to assure completion of any precipitation reactions and structure evolution.

SSDI 0378-7753(94)01977-4

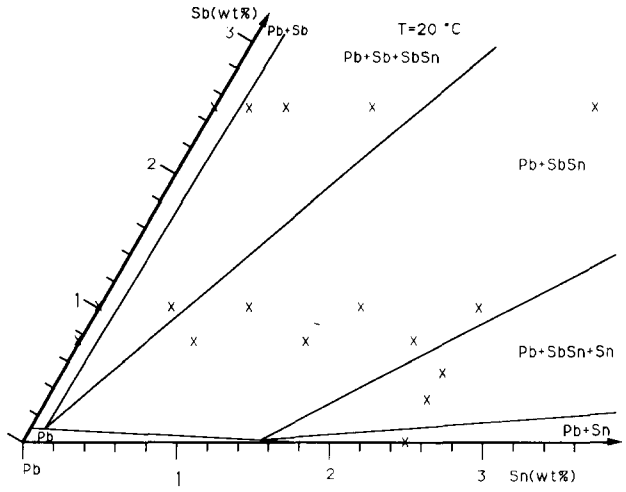

Fig. 1. Composition of different Pb–Sb–Sn alloys.

2.3. Hardness

Vickers hardness (VH) tests were carried out on a Testwell durometer under a load of 2 kg. Each reported value of hardness corresponds to the mean of three points distributed over the entire cross section or the rolled surface of the samples. The empirical relation $HV \approx 0.3\ R$ (MPa) can be used to evaluate the ultimate strength of the alloys.

2.4. Optical microscopy — microprobe analysis

Samples were polished, then etched to reveal the grain structure using a preparatory technique elaborated in our laboratory [7]. This method consists of a cold electrolytic polishing at a temperature of −50 °C (all transformations freezed) followed by repeated chemical etching (following of the boundaries' motion).

3. Results

3.1. Lead–antimony–tin phase diagram

Both Pb–Sb and Pb–Sn systems are simple eutectic diagrams. In the ternary system, four solid phases are observed, namely, Pb, Sb, Sn and Sb–Sn, but no ternary compound exists.

Fig. 2 corresponds to the isothermal section of the ternary system at 240 and 189 °C [8]. At the temperature of rehomogenization, all of our alloys are in the single-phase α-Pb corner.

The limits of the solubilities of antimony and tin at 20 °C are not known very well. For tin, the following values have been reported: 1.9 wt.% [9]; 2–3 wt.% [10]; 1.3 wt.% [11]; 1–2 wt.% [12,13]; and for antimony: 0.17 wt.% at 100 °C [13]. The data in Fig. 1 show the values of 1.9 and 0.1 wt.%, respectively, for the solubilities of tin and antimony at 20 °C. By extrapolation of the

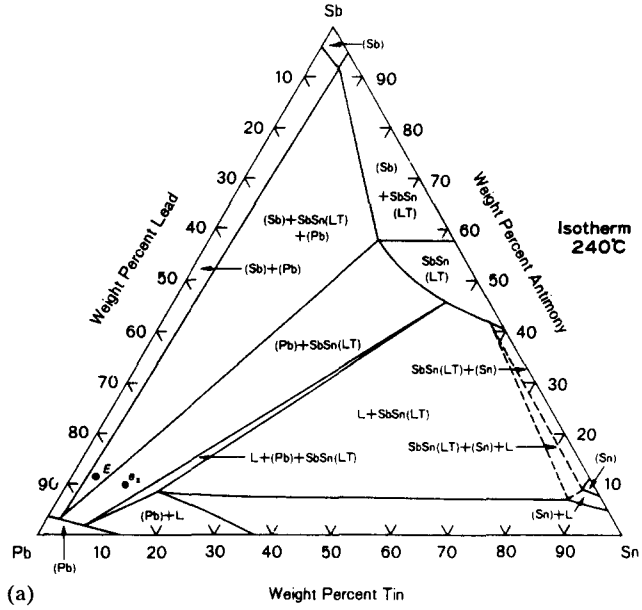

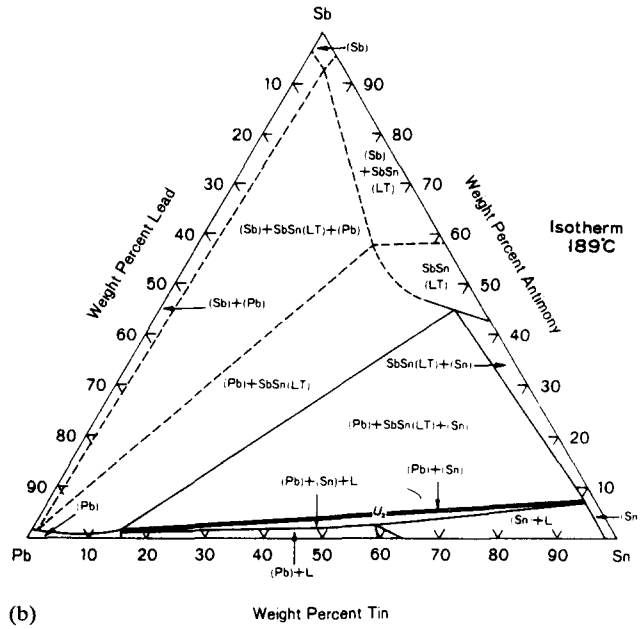

Fig. 2. Isothermal section of Pb–Sb–Sn system at (a) 240 and (b) 189 °C [8].

isothermal section at 240 and 189 °C (Fig. 2(a) and (b)) the different limits of the one-, two- and three-phase domains consistent with our experiments are given. During ageing of the alloys studies here, Sb, SbSn or Sn can precipitate. In a cup at 97.5 wt.% Pb, five domains are crossed from the line PbSb to the line PbSn, viz., Pb + Sb/Pb + Sb + SbSn/Pb + SbSn/Pb + SbSn + Sn/Pb + Sn.

3.2. Structural hardening of alloys

Figs. 3 and 4 show the hardness evolution versus time at 20 °C for different alloys and the three following states: as-cast; rehomogenized; rolled and rehomogenized.

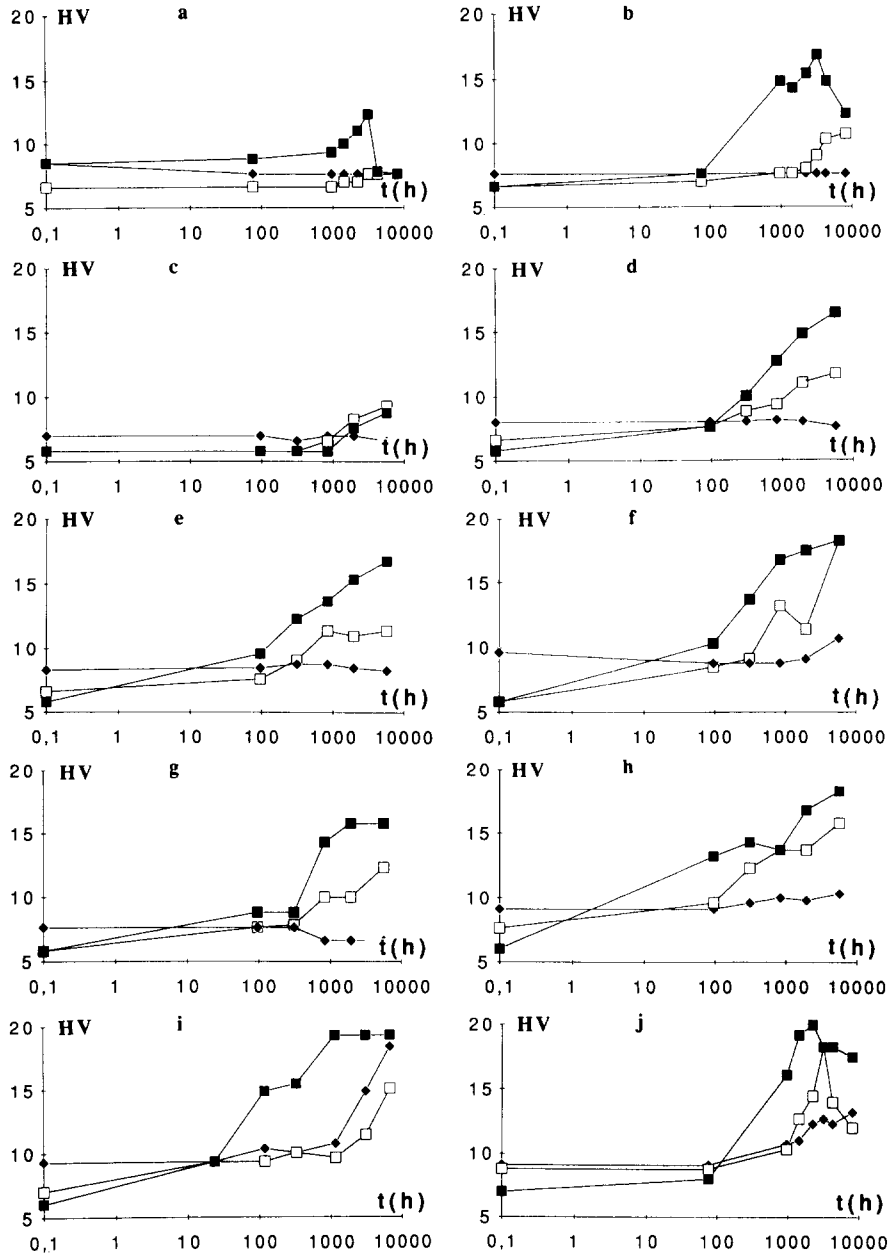

Fig. 3. Hardness evolution vs. time at 20 °C for different alloys (Sb ⩽ 1 wt.%): –◆–, as-cast; –□–, rehomogenized; –■–, rolled and rehomogenized. (a) Pb–0.25wt.%Sb–2.5wt.%Sn; (b) Pb–0.5wt.%Sb–2.5wt.%Sn; (c) Pb–0.75wt.%Sb; (d) Pb–0.75wt.%Sb–0.75wt.%Sn; (e) Pb–0.75wt.%Sb–1.5wt.%Sn; (f) Pb–0.75wt.%Sb–2.2wt.%Sn; (g) Pb–1wt.%Sb; (h) Pb–1wt.%Sb–0.5wt.%Sn; (i) Pb–1wt.%Sb–1wt.%Sn; (j) Pb–1wt.%Sb–1.75wt.%Sn.

3.2.1. As-cast products

With low levels of Sb ($\leqslant$1 wt.%) (Fig. 3), the initial hardness observed is between 7 and 9 HV. The hardening effect is very slight. The microstructures of these alloys consist of large primary dendrites with segregation of antimony at the dendritic sub-boundaries. The solidification segregation reduces the oversaturation of the matrix after casting, cooling and structural hardening. The addition of tin reduces the segregation and increases the oversaturation, but favours the overageing. Indeed, lead–antimony alloys harden through a continuous or generalized precipitation process. An incomplete discontinuous transformation (overageing) follows this continuous precipitation by antimony after one year. But lead–tin alloys present discontinuous precipitation. For the Pb–0.5wt.%Sb–2.5wt.%Sn, Pb–0.75wt.%Sb–2.2wt.%Sn and Pb–1wt.%Sb–2.5wt.%Sn alloys, a discontinuous transformation (Fig. 5) is favoured by the tin content. The transformation starts at the grain boundaries or at the dendritic sub-boundaries. Microprobe analysis shows (in agreement with the diagram given in Fig. 1) that for the Pb–1wt.%Sb–2.5wt.%Sn alloy, only SbSn precipitates. On the other hand, for the Pb–0.5wt.%Sb–2.5wt.%Sn alloy, both SbSn and Sn precipitate. The matrix contains approximately 0.3 wt.% Sb and 2 wt.% Sn, values that are higher than those

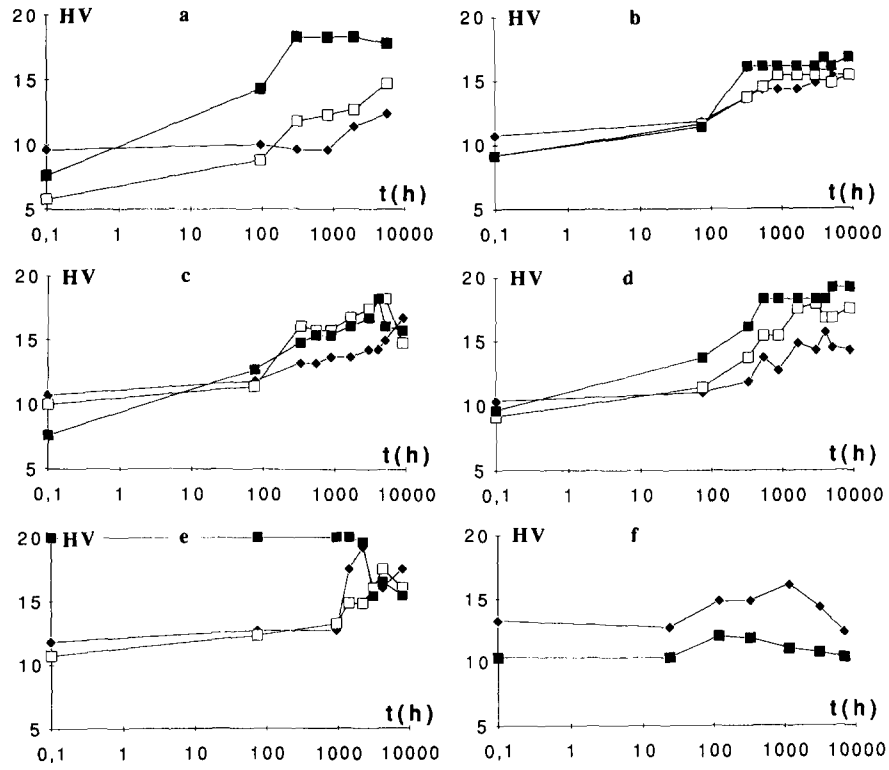

Fig. 4. Hardness evolution vs. time at 20 °C for different alloys (Sb = 2.5 wt.%): -◆-, as-cast; -□-, rehomogenized; -■-, rolled and rehomogenized. (a) Pb–2.5wt.%Sb; (b) Pb–2.5wt.%Sb–0.25wt.%Sn; (c) Pb–2.5wt.%Sb–0.5wt.%Sn; (d) Pb–2.5wt.%Sb–1wt.%Sn; (e) Pb–2.5wt.%Sb–2.5wt.%Sn; (f) Pb–2.5wt.%Sb–4wt.%Sn.

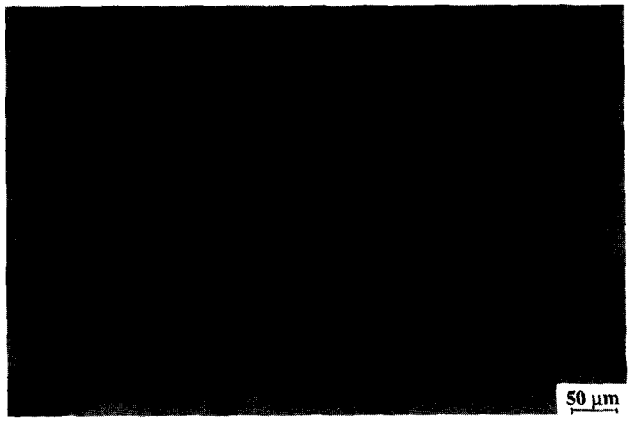

Fig. 5. Discontinuous transformation (overageing) in Pb–0.5wt.%Sb–2.5wt.%Sn alloy after 2 months at 20 °C; as-cast sample.

indicated in the diagram. It would appear that near the large precipitates, finer ones of SbSn (as indicated by microprobe analysis) can still continue to exist in the matrix.

For alloys containing 2.5 wt.% Sb, the initial hardness is greater (9 to 10 HV), see Fig. 4. The final hardness reaches values of 14 HV. The maximum can be greater with an increase of the tin content ($\geqslant$2.5 wt.%), but the discontinuous precipitation (overageing) occurs after some months and provokes a decrease in the hardness.

For alloys containing 2.5 wt.% Sb, segregation is also observed. High levels of antimony and tin, however, allow a good oversaturation of the matrix and a good structural-hardening process.

3.2.2. *Rehomogenized or rolled/rehomogenized samples*

After rehomogenization, the rolled samples display a fine, recrystallized structure. The non-rolled samples retain the large grains of the as-cast product. In no instance, has the casting type of segregation been observed and the initial hardness is lower (6 HV for Sb $\leqslant$ 1 wt.%; 9 HV for Sb = 2.5 wt.%). Thus, the oversaturation is complete and the structural-hardening process is efficient in spite of the medium values of the antimony and tin contents (over 20 HV for alloys with 1 wt.% Sb). Nevertheless, the overageing soon appears for the same reasons.

Theories of the growth process and the morphology of the resulting phase are generally idealized by assuming a plane front of reaction and constant inter-lamellar distances. Experience shows that the growth mechanism is more complex. Several growth directions are observed, e.g., S-shape growths [14,15] at either side of the same boundary, a change in growth orientation with time, etc. In certain cases, the precipitates that result from the discontinuous transformation may become ramified

and change in growth direction under the effect of secondary germinations that develop either on the precipitates or on the transformation front. A difference is also observed between the morphology of SbSn (lamellar) and Sn (rounded form) precipitates (Fig. 6). Microprobe analysis gave the same results as those obtained from the as-cast samples.

3.2.3. Rolled samples

In the case of lead alloys, hardening by cold-work is inefficient as the room temperature corresponds to 0.5 Tf (Tf being the melting temperature in Kelvin degrees) [16,17]. It is generally admitted that under thermal agitation, the hardening defects, and especially the dislocations, introduced by cold-working tend to migrate at a temperature situated between 0.4 and 0.5 Tf (recovery). The structure recrystallizes and gives rise to a softening of the material. The Pb–Ca–Sn alloys with a high Sn/Ca ratio appear to be an exception [18] when the rolling ratio does not exceed 90% [16].

The rolling can be performed before or after ageing. Immediately after rolling, non-aged samples exhibit a higher hardness, see Fig. 7(a). During subsequent treatment at room temperature, the structure changes due to an 'ageing-recrystallization' effect. The end result is the appearance of two opposite mechanisms, namely, a softening one (recrystallization) and a hardening one (continuous precipitation). The initial hardness is higher and the final hardness is lower as the rolling ratio is increased. Optical microscopic examinations confirm that the structure recrystallizes at 20 °C (Fig. 8).

If rolling is performed after hardening (Fig. 7(b)), a slightly harder structure is obtained at first, but this behaviour is very ephemeral. After recrystallization, the final hardness is always lower than that of unrolled samples. With high rolling ratios, the final hardness is often close to that of pure lead.

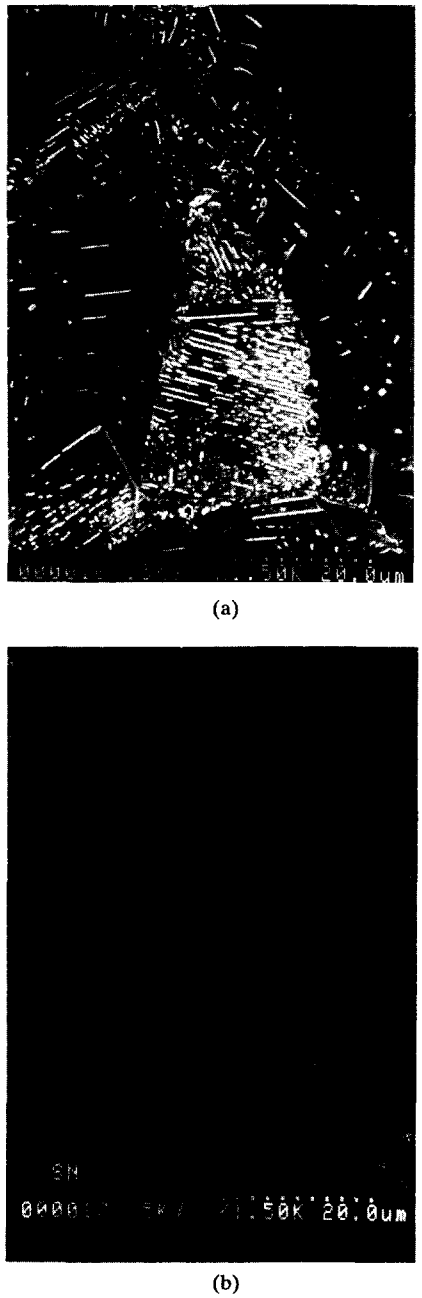

Fig. 6. Discontinuous transformation (overageing) in Pb–0.5wt.%Sb–2.5wt.%Sn alloy after 2 months at 20 °C; rehomogenized sample: (a) electron micrograph; (b) XSn image.

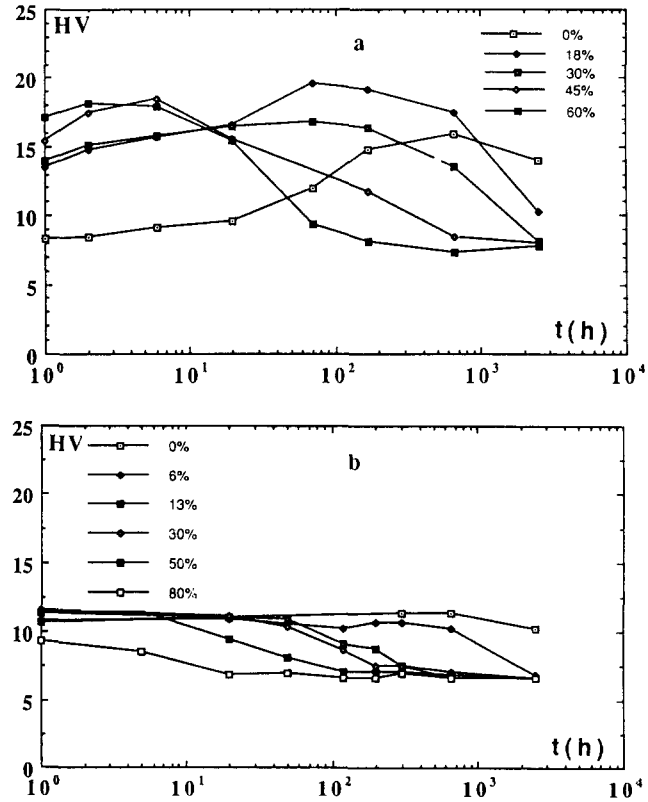

Fig. 7. Hardness evolution vs. time at 20 °C, Pb–2.5wt.%Sb alloy rehomogenized 30 min at 250 °C, water quenched: (a) rolled immediately; (b) rolled after ageing.

Fig. 8. Recrystallization at 20 °C after 80% rolling, Pb–2.5wt.%Sb alloy.

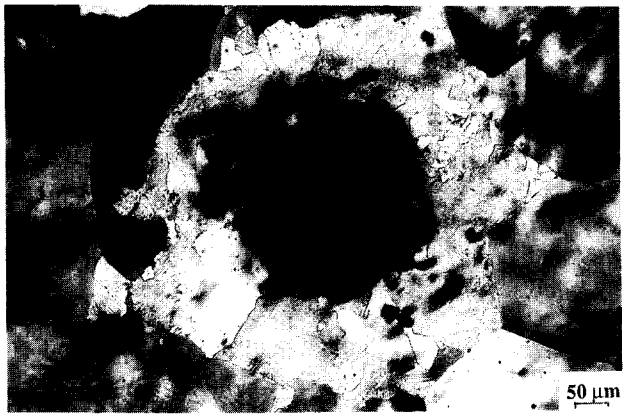

Fig. 9. Discontinuous transformation around a hardness mark, Pb–0.75wt.%Sb–0.75wt.%Sn alloy.

The kinetics of the different continuous and discontinuous transformations are increased by cold-working. The hardness mark induces the discontinuous overageing transformation, as shown in Fig. 9. To restore hardness, the coalesced precipitates have to be redissolved through a rehomogenization at the maximum solubility temperature. After quenching and ageing, the same hardening can be observed as described before.

3.3. Influence of cooling rate and time of rehomogenization

A difference has to be made between the cooling rates of the liquid and the solid. The segregation of antimony and tin, and the morphology of the grains depend on the cooling rate during solidification. In the solid state, a high rate retains the oversaturation of the matrix and prevents precipitation during cooling.

The SiO_2 crucible (diameter 8–10 mm) has been quenched in water at 500 or at 300 °C after air cooling between 500 and 300 °C. After quenching at 500 °C, both the dendritic structure and the segregation are finer, and the initial hardness is a little higher (one to two points).

The necessary time to rehomogenize the alloy depends on the levels of antimony and tin that have been segregated. The alloys (except Pb–2.5wt.%Sb–2.5wt.%Sn and Pb–2.5wt.%Sb–4wt.%Sn) do not show segregation after a rehomogenization of 15 min at 280 °C. For weak levels of antimony and tin, ($Sb + Sn \leqslant 2$ wt.%), a heat treatment of 10 min at 280–290 °C is sufficient.

4. Conclusions

According to the phase diagram, Sb, SbSn or Sn can precipitate during the hardening process in ternary Pb–Sb–Sn alloys. All the alloys harden by continuous precipitation, but tin favours the discontinuous overageing transformation. A difference is observed between the morphology of the new SbSn (lamellar) and Sn (rounded form) precipitates.

The as-cast samples present a dendritic sub-structure with segregation in the sub-boundaries that depends on the cooling rate of the casting. The faster the solidification, the more remote is the structure from the equilibrium diagram [19]. The segregation reduces the oversaturation of the matrix at 20 °C and the hardening of the alloys when the antimony level is low ($\leqslant 1$ wt.%). The addition of tin reduces the segregation and increases the hardening. In this way, tin has a double-action: for $Sb \leqslant 1$ wt.%, a content of 0.5–1 wt.% Sn increases the hardness, but a content of 1.5–2.5 wt.% Sn involves the overageing with a decrease of hardness.

Segregation also occurs in alloys with 2.5 wt.% Sb, but the available amount of antimony in the oversaturated matrix is sufficient for a correct hardening. In this case, small additions of tin exert only minor effects.

After rehomogenization, antimony and tin are dissolved in the matrix after cooling at 20 °C. After ageing, the hardness is higher – even with medium values of antimony and tin. Compared with as-cast samples, the level of tin must be reduced in order to prevent overageing. Finally, the best hardening results are obtained with the Pb–1wt.%Sb–1wt.%Sn alloy (15–19 HV) and corresponds to an ultimate strength of 50–60 MPa.

Hardening by cold-working is inefficient. Under thermal agitation, the hardening defects tend to migrate. The structure recrystallizes. When the rolling ratio is very high, a dynamic recrystallization takes place during the rolling. The driving force of the transformation lies both in the oversaturation of the matrix and in the cold-work energy. By rolling and recrystallization, the coherence of the precipitates is destroyed and the precipitates coalesce. In all cases, the final hardness is always lower than that of unrolled samples.

A rehomogenization, followed by an ageing period, restores the hardness. After this treatment, no segregation and a very fine structure are observed. This behaviour can improve the corrosion resistance, but not necessarily the creep resistance.

References

[1] K. Takahashi, H. Yasuda, K. Yonezu and H. Okamoto, *J. Power Sources, 42* (1993) 221–230.

[2] G. Clerici, *J. Power Sources, 33* (1991) 67–75.

[3] M.D. Achtermann and M.E. Greenlee, *J. Power Sources, 33* (1991) 87–92.

[4] E.M.L. Valeriote, A. Heim and M.S. Ho, *J. Power Sources, 33* (1991) 187–212.

[5] P.S. Kolisnyk and A.M. Vincze, *J. Power Sources, 38* (1992) 59–61.

[6] J. Sklarchuck, M.J. Dewar, E.M. Valeriote and A.M. Vincze, *J. Power Sources, 42* (1993) 47–53.

[7] J.P. Hilger and A. Boulahrouf, *Mater. Charact., 24* (1990) 159–167.

[8] K. Osamura, *Bull. Alloy Phase Diagrams, 6* (1985) 372–379.

[9] M. Hansen and K. Anderko, *Constitution of Binary Alloys,* McGraw-Hill, New York, 2nd edn., 1958.

[10] R.P. Elliot, *Constitution of Binary Alloys,* 1st Suppl., McGraw-Hill, New York, 1965.

[11] F.A. Shunk, *Constitution of Binary Alloys,* 2nd Suppl., McGraw-Hill, New York, 1969.

[12] M.G. Moffatt, *The Handbook of Binary Phase Diagrams,* General Electric Co., Genium Publishing Corporation, Schenectady, NY, USA (continuous updating).

[13] T.B. Massalski, *Binary Phase Diagrams,* American Society for Metals, International Materials Park, OH, USA, 2nd edn., 1990.

[14] R.A. Fournelle, *Acta Metall., 27* (1979) 1135–1155.

[15] M. Frebel and J. Schenk, *Z. Metallk., 70* (1979) 230–240.

[16] J.P. Hilger, *Structural Transformations in Lead Alloys, Training Course COMETT, Nancy, 1993,* Laboratoire de Thermodynamique Métallurgique, Université de Nancy I, ISBN 2 9505958-3-9, VII1–VII43.

[17] J.P. Hilger, *Microstructures et Recristallisation, 34ème Colloque de l'INSTN, Saclay, France, June 21–23, 1994; J. Phys.,* to be published.

[18] H. Borchers and H. Assmann, *Metallwiss. Tech., 33* (1979) 936–941.

[19] B.E. Kallup, D. Berndt and K. Salomon, *Metallwiss. Tech., 37* (1983) 869–873.